8-Hydroxyquinoline complexes (Alq_3) on Al(111): atomic scale structure, energetics and charge distribution

Yann Bulteau,[a] Nathalie Tarrat, †[b] Nadine Pébère[a] and Corinne Lacaze-Dufaure †*[a]

8-Hydroxyquinoline (**8Hq**) is known to efficiently inhibit the corrosion of aluminium by forming metal–organic layers (**8Hq** forms complexes with aluminium atoms). In the present work, the atomic scale structure and the energetics of 8-hydroxyquinoline complexes ($\mathbf{Alq_3}$) adsorbed on an aluminium surface are investigated by dispersion-corrected DFT computations. Two scenarios are considered: (i) an $\mathbf{Alq_3}$ complex, previously formed in vacuum, is deposited on a flat Al(111) surface or (ii) three deprotonated **8Hq** molecules (**q**) directly adsorb on a defective Al(111) surface presenting Al adatoms (Al–Al(111)). For the $\mathbf{Alq_3}$ formation in vacuum, each addition of a **q** molecule on the Al atom stabilises the system, the oxidation state of the Al atom evolving from Al^{I} in **Alq** to Al^{III} in $\mathbf{Alq_2}$ and $\mathbf{Alq_3}$. The subsequent deposition of $\mathbf{Alq_3}$ on Al(111) leads to a strong bonding between the **q** molecules of the complex and the Al(111) surface, with a significant electron transfer occurring from the surface to the complexes (0.73 to 1.57 *e*). The formation on the metal surface of $\mathbf{Alq_3}$ complexes *via* the adsorption of **q** molecules on an Al adatom leads to more stable structures than the ones obtained from direct adsorption of $\mathbf{Alq_3}$ on Al(111). For the most stable adsorption conformation, the three **q** molecules are bonded to the Al adatom but only two are bonded to the aluminium surface. In that case, the total electron transfer from the Al–Al(111) surface to the **q** molecules is 4.40 *e* and the electron transfer from the Al(111) surface to the $\mathbf{Alq_3}$-like species is 2.04 *e*. The structure, energetics and charge distribution data demonstrate an iono-covalent bonding between the **q** molecules and the Al atoms, in the complex as well as on the aluminium surface.

The 8-hydroxyquinoline (**8Hq**, presented in Fig. 1) is a chelating compound commonly used in analytical applications for the detection and removal of metal ions[1] and in other technological fields such as optoelectronics where the deprotonated 8-hydroxyquinoline species (**q**) is combined with aluminium atoms to form highly fluorescent complexes[2–5] ($\mathbf{Alq_3}$) employed for manufacturing organic light emitting diodes (OLEDs).[6–8] The **8Hq** molecule has also been the purpose of numerous studies focused on the corrosion inhibition of aluminium and aluminium alloys and it has been shown to be an highly effective inhibitor.[9–13] In these latter studies, the authors demonstrated that the molecule reacts with aluminium to form metal–organic layers. Indeed, Lamaka *et al.*[10] identified by X-ray photoelectron spectroscopy (XPS) nitrogen-containing layers adsorbed on the Al surface while Soliman *et al.*[12] evidenced, on the basis of Fourier transform infrared spectroscopy (FTIR) and energy-dispersive X-ray spectroscopy (EDX) analyses, the formation on the metallic surface of species combining **8Hq** and Al cations. However, the structure of these metal–organic species deposited on an aluminium surface has not been yet totally characterised at the atomic scale. This is the main aim of the present work.

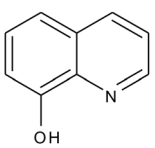

Fig. 1 The **8Hq** molecule.

Experimentally, the deposition under ultrahigh vacuum conditions of $\mathbf{Alq_3}$ complexes on transition metal surfaces (Ag, Cu, Au and Co) has been the subject of several studies.[14–18] Hill *et al.*[14] showed by ultraviolet photoelectron spectroscopy (UPS)

[a] *CIRIMAT, Université de Toulouse, CNRS, INP-ENSIACET, 4 allée Emile Monso, BP44362, Toulouse cedex 31030, France. E-mail: corinne.dufaure@ensiacet.fr; Fax: +33 534323399; Tel: +33 534323412*

[b] *CEMES, Université de Toulouse, CNRS, 29 rue Jeanne Marvig, Toulouse 31055, France*

† These authors contributed equally to this work.

and ellipsometry that the deposition of **Alq_3** complexes on Ag surfaces leads to the formation of polarised molecular layers with an interface dipole. Ino *et al.*[15] investigated the electronic structure of **Alq_3**/Cu and **Alq_3**/Au interfaces by UPS and two-photons photoelectron spectroscopy (2PPE) and showed that **Alq_3** in its ground state interacts weakly with these metal surfaces. Wang *et al.*[16] used scanning tunneling microscopy (STM) to resolve the structure of the first monolayer of **Alq_3** on Cu. At very low coverage, individual **Alq_3** complexes were identified with significant surface mobility. When increasing the surface coverage, pairs and chain-like structures could be resolved, which stability was attributed to direct dipolar and van der Waals interactions. Still on Cu, a combined density functional theory (DFT) and non-contact atomic force microscopy (nc-AFM) study identified intermolecular interactions between **8Hq** in molecular assemblies on the copper surface.[17] Droghetti *et al.*[18] combined desorption, 2PPE studies and electronic structure calculations to conclude that on Co surfaces, one deposited monolayer of **Alq_3** complexes is composed both of chemisorbed (first layer) and physisorbed species, the latter filling the empty spaces.

The adsorption of **8Hq** molecules or **Alq_3** complexes on aluminium surfaces has given rise to only a few experimental and theoretical studies, to our knowledge. Still in the context of ultrahigh vacuum deposition, UPS investigations[19] and non-dispersion-corrected DFT calculations[20] claimed that the electronic properties of free **Alq_3** complexes are preserved upon adsorption on aluminium, suggesting a physisorption of the complexes. Dealing with the interactions between the **Alq_3** complexes and aluminium, Mason *et al.*[21] showed that Al deposition on an **Alq_3** thin film modifies the UPS spectra of the **Alq_3** thin film. The authors concluded that there was a destructive reaction between the **Alq_3** layers and the Al atoms, showing strong chemical interactions. Subsequent DFT work, this time including a van der Waals correction, has highlighted the chemisorption of the **Alq_3** complexes on an Al surface,[22] later confirmed by Yanagisawa *et al.*[23,24] A chemical bonding was also reported from DFT investigations on **Alq_3** complexes adsorbed on cobalt[18,25] and magnesium.[26] In these studies, the presence of a dipole at the organic/metal interface has been evidenced whether the **Alq_3** species is deposited on Al, Co or Mg.

In the framework of corrosion inhibition of aluminium in aqueous solutions, metal–organic species can be formed from **8Hq** crystal dissolved in water. This formation can occur either in solution, the complex already formed subsequently adsorbing on the surface, or directly on the aluminium surface. The direct formation of metal–organic species on metallic surfaces has been previously studied for other corrosion inhibitors, *e.g.* by Kokalj *et al.* for imidazole species[27] or benzotriazole[28] deposited on copper and by Wang *et al.* for alkanethiols adsorbed on gold surfaces.[29] Concerning the **8Hq** species, we demonstrated in previous computational studies that all the species (native **8Hq** molecule, **8Hq** tautomer, deprotonated and protonated **8Hq** species) can chemisorb on Al(111).[30,31] The deprotonated **8Hq** form is the most reactive,[30] leading to the formation of stable and compact organic layers that can inhibit the O_2 reduction reaction on the Al(111) surface.[31] In the present study, we investigate the structure of the metal–organic complexes on an aluminium surface. To this aim, we consider two scenarios: an **Alq_3** complex previously formed in vacuum adsorbs on Al(111) or three **q** molecules directly adsorb on an Al adatom present on the aluminium surface.

In the first part of the paper, computational details are given with a description of the models and the formulas of the different energies discussed in this study. In a second part, the structure, energetics and charge distribution are investigated for **Alq_n** (n = 1, 2 and 3) complexes in vacuum and for **Alq_3** deposited or formed on Al(111). The adsorbed complexes issued from the two scenarios are compared. Finally, the conclusion is presented.

1 Computational details

To investigate the adsorption of 8-hydroxyquinoline species or complexes on aluminium, we have considered the adsorption of dehydrogenated 8-hydroxyquinoline molecules on an Al(111) surface. The term 'dehydrogenated' means hereafter that the O–H bond is dissociated and that the H atom of the hydroxyl group is removed. The choice of the Al(111) surface comes from the fact that, although aluminium develops a protective aluminium oxide thin film on its surface in neutral aqueous solution, this protective film is often defective or partially dissolved due to pH variations, leading to a direct interaction between the species in solution and the bare metallic Al(111) surface. Concerning the molecule, the dehydrogenated 8-hydroxyquinoline radical (Fig. 2) was used to model the deprotonated molecule, these latter corresponding to the **8Hq** form leading to the formation of the complexes. This method is commonly used to investigate the adsorption of anionic molecules on metallic surfaces[27,32–36] in the framework of periodic calculations because it leads to similar results independently of the initial charge on the molecule. In the following, the dehydrogenated 8-hydroxyquinoline molecule will also be noted "**q**".

In this work, we investigate the interaction between **q** molecules and Al atoms within different systems:

(i) **Alq_n** complexes: n **q** molecules (n = 1, 2, 3) in interaction with one Al atom,

(ii) **Alq_3**/Al(111): one **Alq_3** complex adsorbed on a flat Al(111) surface,

(iii) n(**q**)/Al–Al(111): n **q** molecules (n = 1 and 3) in interaction with one Al adatom on an Al(111) surface.

In the following, the Al–Al(111) notation refers to an Al(111) surface with an Al adatom on one hcp site. Total energies were

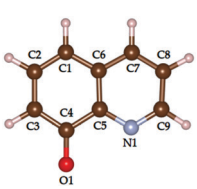

Fig. 2 The **q** molecule. O atom: red ball; N atom: blue ball; C atoms: brown balls; H atoms: white balls.

calculated in the framework of the dispersion-corrected density functional theory (DFT-D). In order to be able to compare our results in vacuum and on surfaces, all the calculations presented in this study were performed using periodic boundary conditions, the latter being necessary to model surfaces. When studying isolated systems, we used simulation boxes large enough to simulate a molecule in vacuum, *i.e.* not affected by its periodic images. Complexation, adsorption, interaction and deformation energies were computed. Negative values for these energies reveal an exothermic process whereas positive values mean an endothermic process. The z direction is the direction normal to the Al(111) surface. Δz value corresponds to the distance between one atom and the average surface plane.

1.1 Isolated $\mathbf{Alq}_n$ complexes (n = 1, 2, 3)

The $\mathbf{Alq}_n$ (n = 1, 2, 3) complexes are composed of one Al atom and n **q** molecules, noted from **A** to **C** (see Fig. 3). To study the isolated **q** molecule and $\mathbf{Alq}_n$ (n = 1, 2, 3) complexes, the species were placed in orthorhombic simulation boxes whose sizes were 22 × 21 × 20 Å^3 for **q** and **Alq**, 32 × 31 × 30 Å^3 for $\mathbf{Alq_2}$ and $\mathbf{Alq_3}$.

In the following equations, E^{X} is the total energy of the optimised system X in vacuum, where X is one Al atom (X = Al), the **q** molecule (X = mol) or an $\mathbf{Alq}_n$ complex (X = cx). The energy $E_{\mathrm{SP}}^{n\mathrm{mol}}$ is the total energy of the isolated system containing n molecules (n = 1, 2, 3) at the geometry in the complex (without the Al atom). Moreover, the energy $E_{\mathrm{SP}}^{\mathrm{moli}}$ is the total energy of the isolated **q** molecule **i** (**i** = **A**, **B**, **C**) at its geometry in the complex.

The complex formation energy is determined from the total energy of the complex E^{cx} from which are subtracted n times the energy of an isolated **q** molecule, n being the number of **q** molecules in the complex, and the energy of an Al atom:

$$E_{\mathrm{form}}^{\mathrm{cx}} = E^{\mathrm{cx}} - nE^{\mathrm{mol}} - E^{\mathrm{Al}} \quad (1)$$

To quantify the interactions in the $\mathbf{Alq}_n$ (n = 1, 2, 3) complex, two interaction energies are calculated:

(i) The interaction energy between the n **q** molecules and the Al atom:

$$E_{\mathrm{int}}^{n\mathrm{mol/Al}} = E^{\mathrm{cx}} - E_{\mathrm{SP}}^{n\mathrm{mol}} - E^{\mathrm{Al}} \quad (2)$$

(ii) The interaction energy between the n **q** molecules.

$$E_{\mathrm{int}}^{\text{inter-mol}} = E_{\mathrm{SP}}^{n\mathrm{mol}} - \sum_{\mathbf{i}=A,\ldots} E_{\mathrm{SP}}^{\mathrm{moli}} \quad (3)$$

For instance, in the case of the $\mathbf{Alq_3}$ complex, the interaction between the three **q** molecules in the complex is equal to:

$$E_{\mathrm{int}}^{\text{inter-mol}} = E_{\mathrm{SP}}^{3\mathrm{mol}} - E_{\mathrm{SP}}^{\mathrm{molA}} - E_{\mathrm{SP}}^{\mathrm{molB}} - E_{\mathrm{SP}}^{\mathrm{molC}} \quad (4)$$

The deformation of the n **q** molecules during the formation of the $\mathbf{Alq}_n$ (n = 1, 2, 3) complex is quantified by:

$$E_{\mathrm{def}}^{n\mathrm{mol}} = \sum_{\mathbf{i}=A,\ldots} E_{\mathrm{SP}}^{\mathrm{moli}} - nE^{\mathrm{mol}} \quad (5)$$

For instance, in the case of the $\mathbf{Alq_3}$ complex, the deformation energy of the three **q** molecules is equal to:

$$E_{\mathrm{def}}^{3\mathrm{mol}} = E_{\mathrm{SP}}^{\mathrm{molA}} + E_{\mathrm{SP}}^{\mathrm{molB}} + E_{\mathrm{SP}}^{\mathrm{molC}} - 3E^{\mathrm{mol}} \quad (6)$$

1.2 Adsorption of the $\mathbf{Alq_3}$ complex on Al(111)

Once the isolated complexes studied, we investigated the adsorption of $\mathbf{Alq_3}$ on an Al surface. To that aim, surfaces were modelled by an asymmetric slab, composed of three Al(111) layers in a 8 × 8 supercell. Periodic images were separated by about 21 Å of vacuum height in the direction normal to the surface to avoid interaction between periodic images in that direction. The $\mathbf{Alq_3}$ complexes were deposited on the top layer of the slab with an empty space of at least 12 Å between the complexes on the surface. The atomic positions of the complex and of the two top layers of the Al slab were unconstrained. The bottom layer of the Al(111) slab was fixed at the bulk positions with a calculated bulk lattice parameter of 4.037 Å (experimental value:[37] 4.05 Å).

In the following equations, E^{X} is the total energy of the optimised system X in vacuum, where X is the $\mathbf{Alq_3}$ complex (X = cx), the Al(111) slab (X = Al(111)), or the $\mathbf{Alq_3}$/Al(111) system (X = cx/Al(111)). In the latter, the $\mathbf{Alq_3}$ complex is adsorbed on the Al(111) surface. $E_{\mathrm{SP}}^{\mathrm{X}}$ (X = cx, Al(111)) is the total energy of the isolated system X constrained at its geometry in the $\mathbf{Alq_3}$/Al(111) system.

To characterise the adsorption on the Al(111) slab of $\mathbf{Alq_3}$ complexes previously optimised in vacuum, the following energy are calculated:

(i) The adsorption energy of the complex on the Al(111) slab:

$$E_{\mathrm{ads}}^{\mathrm{cx/Al(111)}} = E^{\mathrm{cx/Al(111)}} - E^{\mathrm{cx}} - E^{\mathrm{Al(111)}} \quad (7)$$

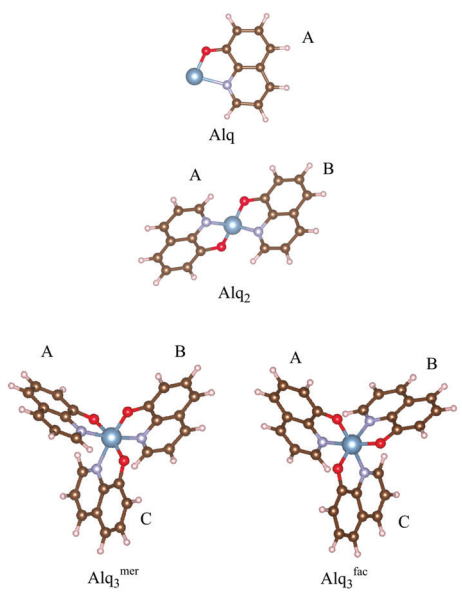

Fig. 3 Isolated $\mathbf{Alq}_n$ (n = 1, 2, 3) complexes. The $\mathbf{Alq_3}$ species exists in meridional (*mer*) and facial (*fac*) isomers. **A**, **B** and **C** indicate the **q** molecules in the complex. Al atoms: big blue balls; O, N, C and H atoms: same colors as in Fig. 2.

(ii) The interaction energy between the complex and the Al(111) slab:

$$E_{\text{int}}^{\text{cx/Al(111)}} = E^{\text{cx/Al(111)}} - E_{\text{SP}}^{\text{cx}} - E_{\text{SP}}^{\text{Al(111)}} \quad (8)$$

(iii) The deformation energy of the adsorbed **Alq$_3$** complex and of the Al(111) slab upon adsorption:

$$E_{\text{def}}^{\text{cx}} = E_{\text{SP}}^{\text{cx}} - E^{\text{cx}} \quad (9)$$

$$E_{\text{def}}^{\text{Al(111)}} = E_{\text{SP}}^{\text{Al(111)}} - E^{\text{Al(111)}} \quad (10)$$

1.3 Adsorption of *n* q molecules (*n* = 1 and 3) on Al–Al(111): *n* q/Al–Al(111) species

Two different systems were investigated, differing by the number *n* of **q** molecules (1 or 3) which were deposited on the Al adatom of the Al(111) slab. The distances between the periodic images of the adsorbed molecules were large enough to avoid any interaction between periodic images.

In the case of the adsorption of three **q** molecules on the adatom, in order to explore the conformations space around an energy minimum, *ab initio* molecular dynamics were performed, followed by DFT optimisations of selected geometries extracted from the MD trajectories. All the details of the MD simulations are given below.

In the following equations, E^{X} is the total energy of the optimised system X, where X is the **q** molecule (X = mol), the Al–Al(111) slab (X = Al–Al(111)), or the system with *n* molecules adsorbed on the Al–Al(111) slab (X = *n*mol/Al–Al(111)). E_{SP}^{X} (X = *n*mol, Al–Al(111)) is the total energy of the isolated system X at the geometry in the *n*mol/Al–Al(111) system.

To characterise the adsorption on the Al–Al(111) slab of *n* **q** molecules, the following energy are calculated:

(i) The adsorption energy of *n* **q** molecules on the Al–Al(111) slab:

$$E_{\text{ads}}^{n\text{mol/Al–Al(111)}} = E^{n\text{mol/Al–Al(111)}} - nE^{\text{mol}} - E^{\text{Al–Al(111)}} \quad (11)$$

(ii) The interaction energy between the *n* **q** molecules and the Al–Al(111) slab:

$$E_{\text{int}}^{n\text{mol/Al–Al(111)}} = E^{n\text{mol/Al–Al(111)}} - E_{\text{SP}}^{n\text{mol}} - E_{\text{SP}}^{\text{Al–Al(111)}} \quad (12)$$

(iii) The interaction energy between two subparts of the system to locally quantify the interactions:

$$E_{\text{int}}^{\text{part1/part2}} = E^{n\text{mol/Al–Al(111)}} - E_{\text{SP}}^{\text{part1}} - E_{\text{SP}}^{\text{part2}} \quad (13)$$

1.4 DFT calculations

DFT calculations were performed using the VASP (Vienna Ab initio Simulation Package) program.[38–40] The PBE exchange correlation functional[41,42] was used. The interactions between electrons and ion cores were described by potentials generated by the Projector augmented-wave method (PAW potentials).[43,44] Dispersion corrections were included, with the addition of a dispersion term to the DFT energy in the Grimme's D2 approach.[45,46] To perform the Brillouin zone integrations, a Monkhorst–Pack sampling[47] of the *k*-points in the reciprocal space was used, *i.e.* a gamma *k*-point sampling for the isolated species and a 2 × 2 × 1 *k*-points sampling for the systems containing an aluminium surface and for the smearing of the Fermi surface, the Methfessel–Paxton method[48] with a width = 0.1 eV was employed. The electronic convergence criterion was 10^{-6} eV with a cutoff energy of 450 eV. For geometry optimisations, the convergence was considered to be reached when forces on atoms were smaller than 5×10^{-3} eV Å^{-1}.

1.5 Geometry exploration by *ab initio* molecular dynamics

In order to explore the conformations space of three **q** molecules adsorbed on Al–Al(111), *ab initio* molecular dynamics were performed (T = 500 K, Langevin thermostat,[49–51] timestep = 1.5 fs, runs of 10 ps, E_{cut} = 300 eV, electronic convergence criterion = 10^{-4} eV, gamma *k*-point sampling). Along the trajectories, only the atoms of the **q** molecules were free to move and the atomic positions of the Al atoms of the Al–Al(111) slab were fixed.

Two initial geometries were chosen. The first one included direct interactions between the molecules and the surface while keeping the O atoms bonded to the adatom (MD1). In the second one, the molecules mainly interacted with the adatom (MD2).

The MD simulations were followed by DFT optimisation of snapshots taken every 320 steps (E_{cut} = 300 eV, electronic convergence criterion = 10^{-4} eV, convergence criterion on forces for optimisation = 5×10^{-3} eV Å^{-1}, gamma *k*-point sampling). The most stable minima (geometry 10 in MD1 and geometry 17 in MD2) were reoptimised with more accurate computational parameters (E_{cut} = 450 eV, electronic convergence criterion = 10^{-6} eV, convergence criterion on forces for optimisation = 5×10^{-3} eV Å^{-1}, 2 × 2 × 1 *k*-points sampling).

1.6 Charge distribution analysis

Atomic net charges were calculated using the Bader population analysis.[52] For a given atom (O, N, C or Al atoms), the atomic net charge is calculated as:

$$\Delta q_{\text{atom}} = -(q_{\text{atom}}^{\text{X}} - q_{\text{atom}}^{\text{isolated}}) \quad (14)$$

where $q_{\text{atom}}^{\text{X}}$ is the number of electrons on the atom in the X species (X = mol, cx, cx/Al(111), mol/Al–Al(111), 3mol/Al–Al(111)) and $q_{\text{atom}}^{\text{isolated}}$ is the number of electrons on the isolated atom.

The electron transfer during the complexation or adsorption is also calculated on the atoms:

$$\Delta q_{\text{atom}} = -(q_{\text{atom}}^{\text{X}} - q_{\text{atom}}^{\text{mol}}) \quad (15)$$

where $q_{\text{atom}}^{\text{mol}}$ is the number of electrons on the atom in the isolated molecule.

On a X species (with X = cx, mol), the total charge transfer upon adsorption ΔQ_{X} is calculated as:

$$\Delta Q_{\text{X}} = Q_{\text{X}} - Q_{\text{X}}^{\text{isolated}} \quad (16)$$

where Q_{X} is the charge on X species in the optimised X/slab system (X = mol or cx and slab = Al(111) or Al–Al(111)) and $Q_{\text{X}}^{\text{isolated}}$ is the charge on the optimised isolated X species.

For one selected case (most stable complex formed on the Al–Al(111) surface), to get more insights into the bonding of the

q molecules on the Al–Al(111) surface, we plot the electron density variation $\Delta\rho$:

$$\Delta\rho = \rho^{n\text{mol/Al–Al(111)}} - \rho_{SP}^{n\text{mol}} - \rho_{SP}^{\text{Al–Al(111)}} \quad (17)$$

where $\rho^{n\text{mol/Al–Al(111)}}$ is the electron density distribution of the optimised *n*mol/Al–Al(111) system, and $\rho_{SP}^{n\text{mol}}$ and $\rho_{SP}^{\text{Al–Al(111)}}$ the electron density distributions respectively of the *n* molecules and the Al–Al(111) slab in vacuum at their geometry after adsorption.

2 Results

In the following, the structure and energetics of the $\mathbf{Alq}_n$ complexes in vacuum are first presented. Then, the structure of $\mathbf{Alq}_3$ complexes on an aluminium surface is investigated within two scenarios: an $\mathbf{Alq}_3$ complex previously formed in vacuum is deposited on a flat Al(111) surface or three **q** molecules directly adsorb on an Al adatom present on the aluminium surface.

2.1 Isolated $\mathbf{Alq}_n$ (n = 1, 2, 3) complexes

$\mathbf{Alq}_n$ complexes can be formed by interaction between n **q** molecules and one Al atom. For n = 3, the $\mathbf{Alq}_3$ complex exists in two isomers: meridional, noted $\mathbf{Alq}_3^{\text{mer}}$, and facial, noted $\mathbf{Alq}_3^{\text{fac}}$.[2,53,54] In the meridional isomer, the O atoms form a plane that is almost perpendicular to the plane formed by the N atoms. In the facial isomer, O atoms and N atoms belong to two planes almost parallel and the O atoms are directed to one side of the complex while the N atoms are directed to the opposite side. It has been shown that the meridional isomer is more stable in aqueous solution that the facial one.[2,53,54] In order to investigate the interactions in these complexes, we performed calculations on systems composed of one Al atom and one to three **q** molecules, *i.e.* **Alq**, $\mathbf{Alq}_2$ and $\mathbf{Alq}_3$ complexes. The optimised geometries are presented in Fig. 3. It was not possible to place four or more molecules around the aluminium atom due to steric hindrance.

Energies calculated for the optimised complexes are presented in Table 1, O–Al and N–Al bond lengths in Table 2, and net charges on the atoms and charges variation upon complexation in Table 3.

The formation energy $E_{\text{form}}^{\text{cx}}$ takes into account the interaction energy $E_{\text{int}}^{n\text{mol/Al}}$ between the n **q** molecules and the Al atom, the variation of the internal energy of the n molecules due to the deformation occurring during the complexation $E_{\text{def}}^{n\text{mol}}$ and the interaction energy between the n **q** molecules $E_{\text{int}}^{\text{inter-mol}}$ in the resulting complex, *i.e.* $E_{\text{form}}^{\text{cx}} = E_{\text{int}}^{n\text{mol/Al}} + E_{\text{def}}^{n\text{mol}} + E_{\text{int}}^{\text{inter-mol}}$. The $\mathbf{Alq}_n$ (n = 1, 2, 3) complexes formation is highly stabilising, with complex formation energies per molecule ranging from −4.54 eV for $\mathbf{Alq}_3^{\text{fac}}$ to −4.99 eV for **Alq**. The **q** molecules are strongly bonded to the Al atom, proof of this being the interaction energy between the **q** molecules and the Al atom which ranges from −5.02 eV per molecule for $\mathbf{Alq}_3^{\text{fac}}$ to −5.39 eV for $\mathbf{Alq}_2$. The van der Waals contribution to these energies is low (1.4–5.2% for the formation energies and below 1.5% for the interaction energies), this contribution increasing with the number of **q** molecules. The calculated interaction energies between the **q** molecules in the complexes $E_{\text{int}}^{\text{inter-mol}}$ are positive (0.24 to 0.61 eV) and show globally repulsive interactions between them, despite the attractive van der Waals contribution. Concerning the structure of the complexes, the O–Al bonds are shorter than the N–Al bonds (1.844 ± 0.074 Å and 2.051 ± 0.154 Å respectively) in all the complexes, and these values are in agreement with previous theoretical[24] and experimental[2,3,55] studies. The shorter bond lengths in the $\mathbf{Alq}_2$ species, which has a symmetric structure, show stronger O–Al and N–Al interactions than in the other $\mathbf{Alq}_n$ species. The geometrical and energetic properties of the $\mathbf{Alq}_2$ species are different from the ones of the other complexes with a stronger deformation of the molecules (0.52 eV per molecule for $\mathbf{Alq}_2$ *versus* 0.36 eV and 0.29 ± 0.01 eV for **Alq** and $\mathbf{Alq}_3$) and a strong repulsion between them ($E_{\text{int}}^{\text{inter-mol}}$ = 0.24 eV).

The oxidation state of the aluminium atom varies when evolving from one to two complexed **q** molecules but remains stable when a third molecule is added. Indeed, the charge on the Al atom in the complexes is +0.86 *e* in **Alq** and +2.43 ± 0.02 *e* in $\mathbf{Alq}_2$ and $\mathbf{Alq}_3$ (Table 3). It shows that the Al atom ($3s^2 3p^1$) tends to be in Al^{I} or Al^{III} oxidation states in the **Alq** and $\mathbf{Alq}_n$ (n = 2, 3) complexes, respectively. This significant change in the aluminium electronic structure occurring when n goes from 1 to 2 is reflected by a higher variation of the interaction energy upon the addition of an other **q** molecule when going from **Alq**

Table 2 Bond lengths (in Å) in the $\mathbf{Alq}_n$ (n = 1, 2, 3) complexes (shown in Fig. 3)

	molA		molB		molC	
Species	$d_{\text{O–Al}}$	$d_{\text{N–Al}}$	$d_{\text{O–Al}}$	$d_{\text{N–Al}}$	$d_{\text{O–Al}}$	$d_{\text{N–Al}}$
Alq	1.848	2.187				
$\mathbf{Alq}_2$	1.770	1.897	1.770	1.897		
$\mathbf{Alq}_3^{\text{mer}}$	1.891	2.039	1.860	2.052	1.888	2.092
$\mathbf{Alq}_3^{\text{fac}}$	1.856	2.097	1.855	2.099	1.856	2.103

Table 1 Formation energies of the $\mathbf{Alq}_n$ (n = 1, 2, 3) complexes and van der Waals energy contribution, formation energies per molecule, interaction energies between the **q** molecules and the Al atom and van der Waals energy contribution, interaction energies per molecule, interaction energies between the **q** molecules and van der Waals energy contribution and total deformation energies of the n molecules (in eV)

Species	$E_{\text{form}}^{\text{cx}}$	$E_{\text{form}}^{\text{cx}}$(vdW)	$E_{\text{form}}^{\text{cx}}/n$	$E_{\text{int}}^{n\text{mol/Al}}$	$E_{\text{int}}^{n\text{mol/Al}}$(vdW)	$E_{\text{int}}^{n\text{mol/Al}}/n$	$E_{\text{int}}^{\text{inter-mol}}$	$E_{\text{int}}^{\text{inter-mol}}$(vdW)	$E_{\text{def}}^{n\text{mol}}$
Alq	−4.99	−0.07	−4.99	−5.35	−0.07	−5.35			0.36
$\mathbf{Alq}_2$	−9.51	−0.21	−4.75	−10.79	−0.14	−5.39	0.24	−0.09	1.04
$\mathbf{Alq}_3^{\text{mer}}$	−13.74	−0.64	−4.58	−15.20	−0.22	−5.07	0.56	−0.45	0.90
$\mathbf{Alq}_3^{\text{fac}}$	−13.62	−0.71	−4.54	−15.06	−0.22	−5.02	0.61	−0.52	0.83

Table 3 Net charges q_{atom} and charge variations Δq_{atom} (in e) on the Al, O and N atoms during the formation of **Alq$_n$** (n = 1, 2, 3) complexes

	Al	mol**A**		mol**B**		mol**C**	
Species	(q_{Al})	q_O (Δq_O)	q_N (Δq_N)	q_O (Δq_O)	q_N (Δq_N)	q_O (Δq_O)	q_N (Δq_N)
Isolated **q**		−0.96	−1.15				
Alq	+0.86	−1.31 (*−0.35*)	−1.37 (*−0.22*)				
Alq$_2$	+2.41	−1.30 (*−0.34*)	−1.42 (*−0.27*)	−1.30 (*−0.34*)	−1.42 (*−0.27*)		
Alq$_3^{mer}$	+2.45	−1.35 (*−0.39*)	−1.33 (*−0.18*)	−1.35 (*−0.39*)	−1.27 (*−0.12*)	−1.26 (*−0.30*)	−1.27 (*−0.12*)
Alq$_3^{fac}$	+2.45	−1.25 (*−0.29*)	−1.34 (*−0.19*)	−1.25 (*−0.29*)	−1.36 (*−0.21*)	−1.26 (*−0.30*)	−1.36 (*−0.21*)

to **Alq$_2$** (−5.44 eV) than when going from **Alq$_2$** to **Alq$_3$** (−4.27 and −4.41 eV for the *fac* and *mer* isomers respectively). The electron transferred by the aluminium atom are located more on the oxygen atoms (0.29 to 0.39 e) than on the nitrogen ones (0.12 to 0.27 e).

This study of the **Alq$_n$** (n = 1, 2, 3) complexes in vacuum shows that the system is stabilised by each addition of a **q** molecule on the Al atom. When three molecules are complexed to the Al atom, the **Alq$_3^{mer}$** isomer is found to be the most stable one by 120 meV,‡ close to the value of 210 meV calculated by Lima *et al.* (M06-2X/6-31+G(d,p)/SDD level of theory).[3] High electrons transfers are observed from the Al atom to the molecules upon complexation with two oxidation states of the Al atom in the systems (Al^{I} in Alq and Al^{III} in **Alq$_2$** and **Alq$_3$**). It leads to a strong bonding between the Al atom and the **q** molecules. As experimental works proposed that **q** complexes are present on aluminium surfaces during the corrosion inhibition process by **8Hq** molecules,[9–13] the adsorption of complexes on the Al(111) surface was investigated and the results are presented in the following. First, the deposition on Al(111) of an **Alq$_3$** complex previously formed in vacuum was studied.

2.2 Alq$_3$ complexes on an aluminium surface

2.2.1 Adsorption of Alq$_3$ complexes on the flat Al(111). The **Alq$_3^{fac}$** and the **Alq$_3^{mer}$** complexes were absorbed on an Al(111) surface. For both *mer* and *fac* isomers, initial geometries were chosen so that O and N atoms are directed towards the aluminium surface, in order to favour the bonding between the complex and the surface. When the complex is adsorbed on the Al(111) surface, it can access two configurations, *i.e.* an upward configuration, denoted by '*up*' hereafter, and a downward configuration, designed by '*down*' hereafter. These notations are the ones proposed by Yanagisawa *et al.*[24] who characterised the adsorption modes relatively to the molecular permanent dipole. The latter is directed to the vacuum side for the *up* configuration while it is directed to the substrate in the *down* configuration. The *mer/up*, *mer/down*, and the *fac/up* adsorption modes are show in Fig. 4. The *fac/down* orientation was not investigated because it has been shown to be the least stable one.

The coverage θ of the Al(111) surface by the adsorbed complexes is defined as the number of surface Al atoms covered by the complexes $n_{Al}^{covered}$ divided by the total number of Al surface atoms in the supercell ($n_{Al}^{surface}$ = 64 atoms). A complete surface coverage (θ = 1 ML) corresponds to the case in which all surface Al atoms are covered by the complexes. As the **Alq$_3^{fac}$** and the **Alq$_3^{mer}$** complexes do not have the same geometrical form and can adsorb in an *up* or *down* position, their adsorption lead to the coverage of different numbers of surface Al atoms. Thus, $\theta = n_{Al}^{covered}/n_{Al}^{surface}$ = 0.16 ML, 0.19 ML and 0.20 ML for the *fac/up*, *mer/up* and *mer/down* conformations respectively.

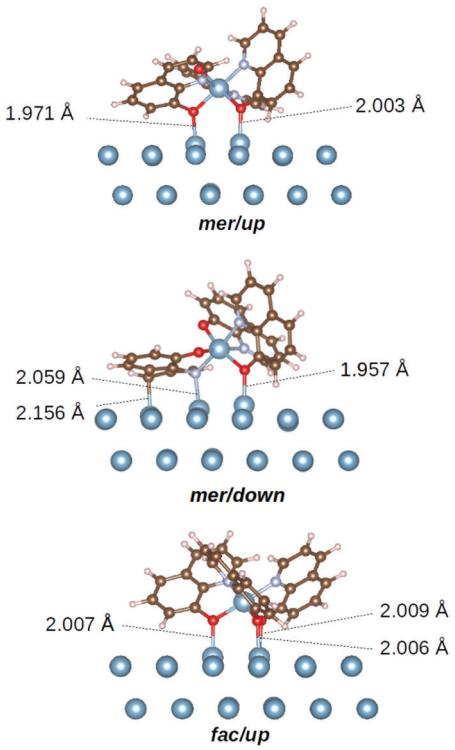

Fig. 4 **Alq$_3$** complexes adsorbed on an Al(111) surface. Top: Meridional up (*mer/up*). Middle: Meridional down (*mer/down*). Bottom: Facial up (*fac/up*); for practical purposes, only two layers of the Al(111) slab are shown.

The adsorption energies of the **Alq$_3$** complexes on the Al(111) surface, the interaction energies, and the complex and Al(111) slab deformation energies are summarised in Table 4, together with the distances between the Al atom of the complex and the aluminium surface, the net charges on the Al atom of the complex and the charge variations due to adsorption.

The *fac/up* configuration is the most stable one, with the three O atoms of the **Alq$_3$** complex bonded to the Al surface (top positions, d_{O-Al} = 2.007 ± 0.002 Å). This is consistent with

‡ The geometries of the *fac* and *mer* isomers were reoptimised employing an implicit solvation model (implemented in the VASP code) to simulate the effects of the aqueous solution. Both isomers were found to be isoenergetic in solution, with a *fac*/*mer* populations ratio of 50/50. The adsorption of both the *fac* and *mer* isomers was thus considered in the following.

Table 4 **Alq_3** complexes adsorbed on an Al(111) surface. Relative total energies (the reference is the total energy of the *fac/up* configuration), adsorption energies of the **Alq_3** complexes on the Al(111) surface, interaction energies, complex and Al(111) slab deformation energies (in eV), distance between the Al atom of the complex and the Al(111) surface (in Å), net charge on the Al atom of the complex and charge variation on the complex upon adsorption (in *e*)

	$\Delta E^{cx/Al(111)}$	$E_{ads}^{cx/Al(111)}$	$E_{int}^{cx/Al(111)}$	E_{def}^{cx}	$E_{def}^{Al(111)}$	d_z(Al)	q_{Al}	ΔQ_{cx}
mer/up	0.54	−1.68	−3.12	0.88	0.56	3.862	+2.44	−0.73
mer/down	0.69	−1.52	−4.25	2.09	0.63	3.897	+2.36	−1.57
fac/up	0	−2.21	−3.45	0.73	0.51	3.509	+2.45	−0.97

the previous works on the adsorption of **Alq_3** on Al(111)[24] and on Co(111).[18,25] The *fac/up* configuration is energetically followed by the *mer/up* and *mer/down* configurations that are higher in energy by 0.54 and 0.69 eV, respectively. In the *mer/up* configuration, the **Alq_3** complex is bonded to the surface by two O atoms (top positions, $d_{O–Al}$ = 1.971 Å and 2.003 Å) whereas in the *mer/down* configuration, the **Alq_3** complex bonds to the Al(111) surface by one O atom, one N atom, and one C atom (top positions, $d_{O–Al}$ = 1.957 Å, $d_{N–Al}$ = 2.059 Å and $d_{C–Al}$ = 2.156 Å).

The complexes are strongly in interaction with the Al(111) surface with values ranging from −1.52 eV to −2.21 eV for the adsorption energies of the **Alq_3** complexes on the Al(111) surface and −3.12 to −4.25 eV for the interaction energies. The Al(111) surface is deformed in the adsorption zone ($E_{def}^{Al(111)}$ = 0.57 ± 0.06 eV), and it is also the case for the complexes which deform in order to optimise their interaction with the surface. The deformation energies of the complexes are much lower for the *up* configurations (0.81 ± 0.07 eV) than for the *mer/down* one (2.09 eV) in which the bonding of the O, C, and N atoms with the surface induced a strong deformation. The *mer/down* configuration is thus the less stable adsorption mode (−1.52 eV) even if its complex-surface interaction energy is the strongest one (−4.25 eV).

The distance between the Al atom in the complex and the Al(111) surface is above 3.5 Å and the charge on the Al atom in the complex remains unchanged upon adsorption for the *fac/up* and *mer/up* configurations and is very slightly modified for the *mer/down* configuration (Δq_{Al} = −0.09 *e*). Whatever the complex, an electron transfer occurs during adsorption, the electrons moving from the metal surface to the complex. The largest transfer takes place for the *mer/down* configuration (1.57 *e*), this significant charge transfer inducing, as explained above, strong complex–surface interactions and molecule deformation.

To investigate the stability of the adsorption of the **Alq_3** complex on the Al(111) surface at ambient (300 K) and high (500 K) temperatures, molecular dynamics runs of 3 ps were performed for the *fac/up* configuration. The system stayed in a similar *fac/up* geometry for all the duration of the runs without breaking of O–Al bonds.

To summarise, we showed by depositing the **Alq_3** complexes pre-formed in vacuum on the aluminium surface, that the most stable configuration is the *fac/up* one. Following the second scenario, which consists of the direct adsorption of three **q** molecules on an adatom of the aluminium surface, the formed complex could be more stable. In the next section we explore this path.

2.2.2 Direct formation of an Alq_3 complex on an Al–Al(111) surface. In the following paragraph, the adsorption of one **q** molecule on the Al–Al(111) surface is investigated, followed by the one of three **q** molecules. In all systems, the Al adatom is located on a threefold hcp site of the Al(111) surface as it was found to be 46 meV more stable than on a threefold fcc site. In that case, the adatom lies at 2.034 Å perpendicularly to the Al(111) surface plane and has a net charge of +0.12 *e*. For comparison, the DFT-D calculated Al(111) interlayer distance in the bulk is 2.314 Å.

*2.2.2.1 One **q** molecule adsorbed on Al–Al(111).* Two adsorption modes for a **q** molecule on Al–Al(111) were studied in which the molecule is either parallel or perpendicular to the surface. The geometry optimisations lead to two stable geometries, presented in Fig. 5. In the most stable one, the **q** molecule is parallel to the Al(111) surface and is bonded both to the Al adatom ($d_{O–Al}$ = 1.927 Å, $d_{N–Al}$ = 1.914 Å) and to the Al(111) surface ($d_{O–Al}$ = 2.051 Å, $d_{C–Al}$ = 2.209 Å). In the perpendicular structure, which lies 0.13 eV higher in energy (Table 5), the molecule is only bonded on top of the adatom ($d_{O–Al}$ = 1.813 Å, $d_{N–Al}$ = 1.998 Å). In both cases, the **q** molecule is thus strongly bonded to Al–Al(111) with adsorption energies of −4.10 ± 0.07 eV (in Table 5). For comparison, DFT-D adsorption energies of a single **q** molecule on a perfect Al(111) surface were computed and are −3.61 eV and −3.48 eV for a tilted and a parallel adsorption mode, respectively. The comparison of the adsorption energies thus indicates that the bonding of a **q** molecule on Al–Al(111) is stronger than its bonding on a flat Al(111) surface. The complex formed on the surface in the parallel adsorption mode is stabilised by the very strong interaction between the molecule and the Al–Al(111) surface (−6.14 eV for the interaction energy to be compared to −5.35 eV

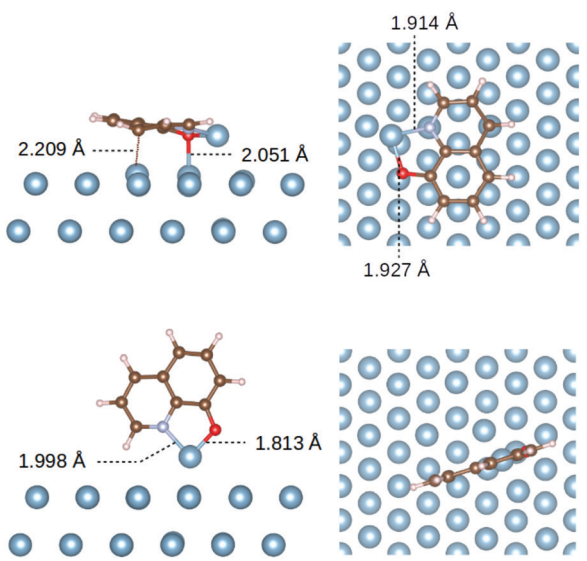

Fig. 5 One **q** molecule adsorbed on Al–Al(111). Top: Parallel adsorption mode. Bottom: Perpendicular mode.

Table 5 One **q** molecule adsorbed on Al–Al(111). Adsorption energies, interaction energies, molecule and Al–Al(111) surface deformation energies (in eV), distance (distance variation) between the Al adatom and the surface (in Å), net charge on the Al adatom (charge variation), charge variation on the **q** molecule upon adsorption (in *e*)

Species	$E_{ads}^{mol/Al-Al(111)}$	$E_{int}^{mol/Al-Al(111)}$	E_{def}^{mol}	$E_{def}^{Al-Al(111)}$	z_{Al} (Δz_{Al})	q_{adatom} (Δq_{adatom})	ΔQ_{mol}
Parallel geometry	−4.17	−6.14	1.42	0.55	2.407 (+0.373)	+0.82 (+0.70)	−2.11
Perpendicular geometry	−4.04	−4.57	0.40	0.14	1.981 (−0.054)	+1.03 (+0.91)	−0.95

for the **Alq** complex in vacuum) whereas the **q** molecule is less bonded to the Al atoms for the perpendicular adsorption mode (−4.57 eV for the interaction energy).

The **q** molecule is highly deformed in its parallel adsorption mode (1.42 eV for the deformation energy) as well as the Al–Al(111) surface which has a significant deformation energy (0.55 eV) due to a local deformation of the surface plane and the displacement of the adatom (+0.373 Å) which has occurred during the molecule adsorption. This is a first insight into the formation of an **Alq** species on the Al surface. For the perpendicular mode, the **q** molecule and the Al–Al(111) slab are much less deformed (0.40 eV and 0.14 eV) and the distance between the adatom and the Al(111) surface is only slightly decreased (−0.054 Å).

For both adsorption modes, the Al adatom is in its Al^{I} oxidation state with a net charge of +0.82 *e* and +1.03 *e*, similarly to the case of the isolated **Alq** complex. These results show that the **q**-Al adatom part of the system behaves as the isolated **Alq** complex.

For the parallel adsorption mode, there is an electron transfer of 2.11 *e* from the metal to the **q** molecule. These electrons come from the atoms of the surface plane and from the Al adatom, which undergoes a charge variation of 0.70 *e*. For the perpendicular geometry, the **q** molecule gains 0.95 *e* that comes from the Al adatom. When a **q** molecule is adsorbed on a perfect Al(111) surface, the electron transfer from the Al(111) surface to the molecule is 1.92 *e* and 1.20 *e* for the parallel and tilted adsorption modes, respectively. Thus, for the parallel adsorption of the **q** molecule, the additional bonding to the adatom increases by 0.2 *e* the electron transfer to the molecule. The comparison of the tilted adsorption on Al(111) and the perpendicular adsorption on Al–Al(111) is less obvious since the molecule is further from the surface when adsorbed on the adatom.

We demonstrated that the bonding of one **q** molecule on the Al–Al(111) surface is strong and that the parallel and perpendicular adsorption modes are close in energy, due to a balance between interaction and deformation energies. In the following paragraph, we investigate the adsorption of three **q** molecules on Al–Al(111).

*2.2.2.2 Three **q** molecules adsorbed on Al–Al(111).* To explore the conformations space of a system containing 3 **q** molecules adsorbed on the Al–Al(111) surface, we performed two *ab initio* molecular dynamics runs (MD1 and MD2) differing by their starting geometry. In the initial geometry of MD1, the three **q** molecules were adsorbed parallel to the surface and bonded to the Al adatom, while for MD2 two **q** molecules lied parallel to the surface and bonded to the adatom and the third one was located on top of the Al adatom.

Twenty geometries were extracted along each MD trajectory and optimised. Some selected distances are depicted in Fig. 6 for the structures issued from MD1 and in Fig. 7 for the ones issued from MD2 and the associated energies are shown in Fig. 8 and 9, together with the number of bonds existing between the **q** molecules and the Al–Al(111) surface.

Three O–Al adatom bonds are present in all the structures, whether they come from MD1 (Fig. 6(b)) or MD2 ((Fig. 7(a)). As there is no change in the number of these bonds, there are not presented in Fig. 8 and 9. Fig. 6 shows variations of the position and orientation of the three molecules (namely **A**, **B** and **C**), relatively to the adatom and to the surface Al atoms along the MD1 trajectory. Concerning the O atoms, additionally to the bonding with the Al adatom, one or two O–surface Al bonds are formed (Fig. 6(c)). The N atom of each molecule is bonded or not to the adatom (Fig. 6(d)) and to an Al atom of the surface (Fig. 6(e)), depending on the geometry. Finally, the variation of the distance between the C7 atom in the molecules and one surface Al atom (Fig. 6(f)) shows that the molecules move and can be also bonded to the surface *via* a C–Al bond (geometry 17). In Fig. 8, the total energy of the system is depicted relatively to the most stable one issued from MD1 (geometry 10). The values seem to be split into two groups: one corresponding to the lowest energies (geometries 1–2, 9–13, 15 and 17) and one corresponding to higher energies (geometries 3–8, 14, 16, 18–20). The energies of these two groups are different of at least 0.2 eV. For the most stable geometries, except for geometries 1 and 2, two O–surface Al atoms bonds are present. Moreover, one N–Al adatom and one or two N–surface Al bonds are formed. An exception is geometry 17, which has a low energy despite the absence of N–adatom bond. This latter seems to be compensated for by the presence of a bond between the Al surface and the C7 atom of molecule **C**.

The structures extracted from the MD2 trajectory differ much less than those from MD1. Indeed, the evolution of the selected distances depicted in Fig. 7 shows few variations of the position and orientation of the three molecules **A**, **B** and **C**, relatively to both the Al adatom and the surface. Two O atoms are always bonded to the surface (Fig. 7(b)), two N atoms to the adatom (Fig. 7(c)), and one N atom to the surface (Fig. 7(d)). The only significant variations are related to the bonding between C atoms of the molecules and Al atoms of the surface (Fig. 7(e) and (f)). In Fig. 9, the energy is plotted relatively to the most stable form issued from MD2 (geometry 17). The energies are in a very small range (< 0.05 eV), except for geometries 2, 17 and 18. The geometry 2 is the less stable one. In that geometry,

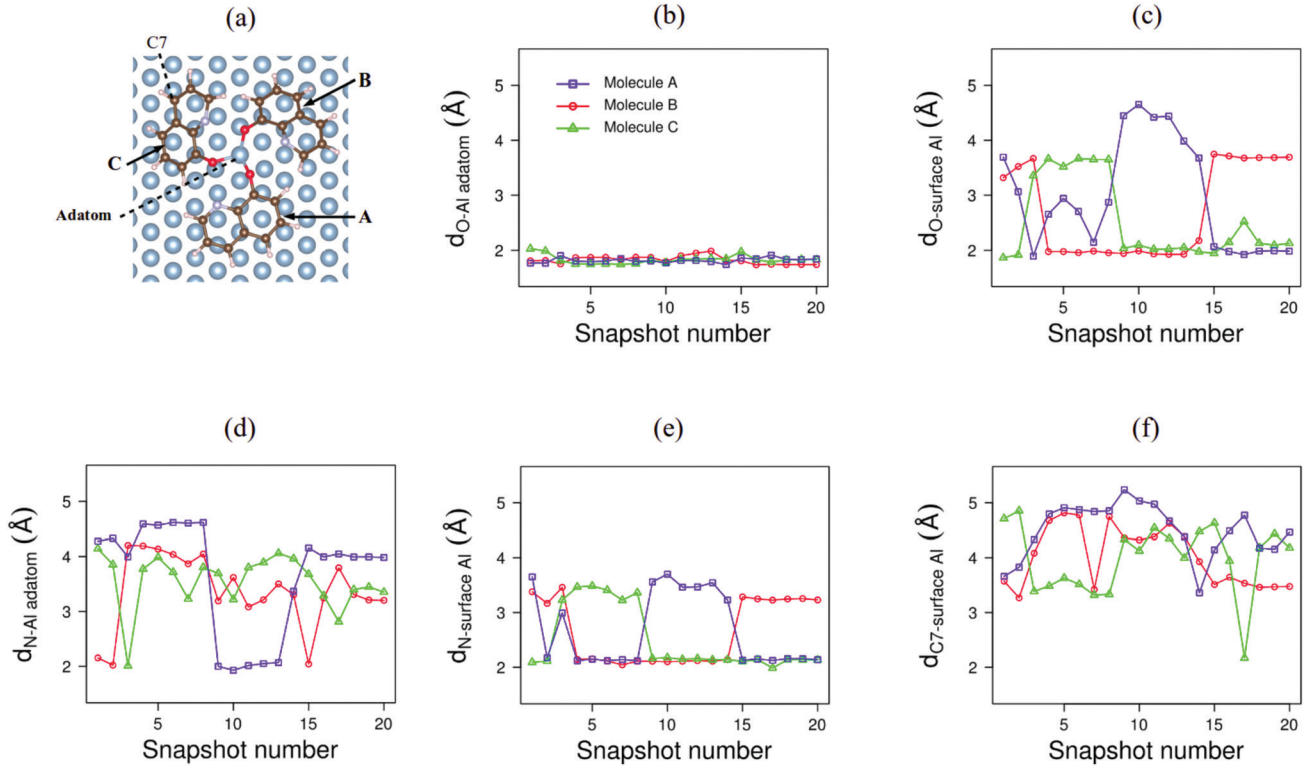

Fig. 6 Three **q** molecules adsorbed on Al–Al(111). Geometries optimised from 20 snapshots of MD1; (a) atom numbering; distances (in Å) (b) between the O atom and the Al adatom, (c) between the O atom and a surface Al atom (shortest distances), (d) between the N atom and the Al adatom, (e) between the N atom and a surface Al atom (shortest distances), (f) between the C7 atom and a surface Al atom (shortest distances). Data for molecules **A** in blue, **B** in red and **C** in green.

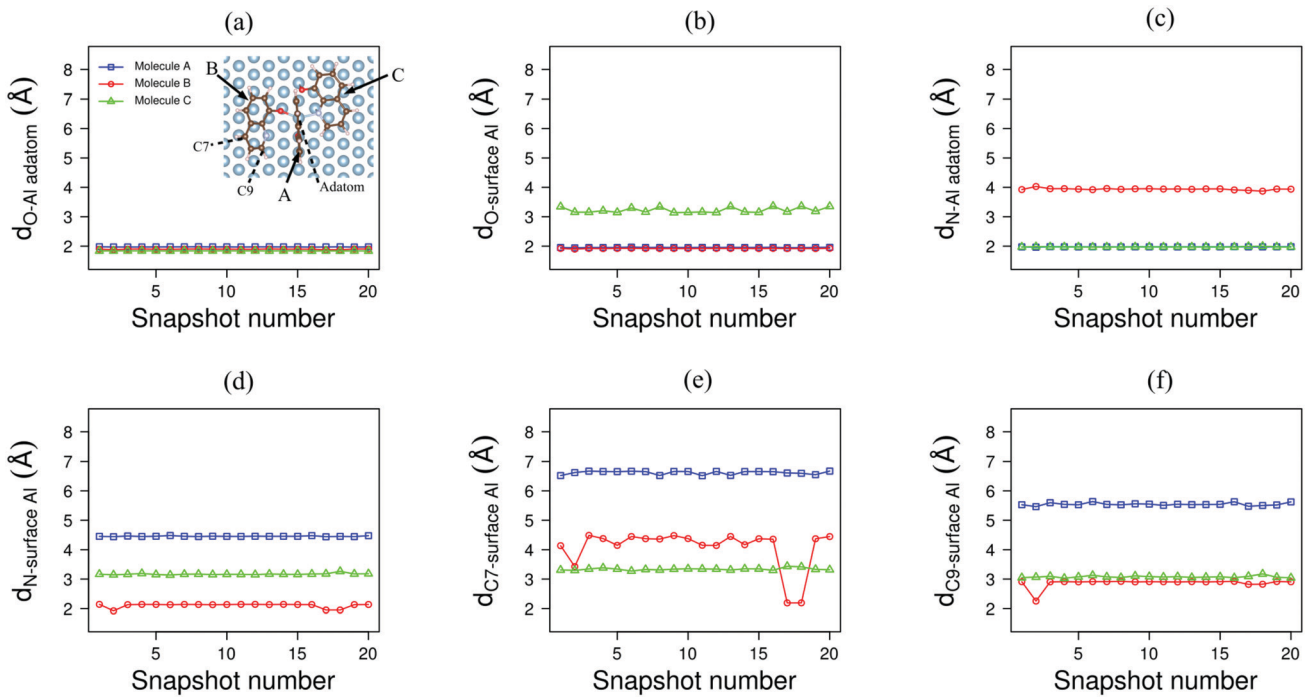

Fig. 7 Three **q** molecules adsorbed on Al–Al(111). Geometries optimised from 20 snapshots of MD2; for atom numbering, see inset; distances (in Å) (a) between the O atom and the Al adatom, (b) between the O atom and a surface Al atom (shortest distances), (c) between the N atom and the Al adatom, (d) between the N atom and a surface Al atom (shortest distances), (e) between the C7 atom and a surface Al atom (shortest distances), (f) between the C9 atom and a surface Al atom (shortest distances). Data for molecules **A** in blue, **B** in red and **C** in green.

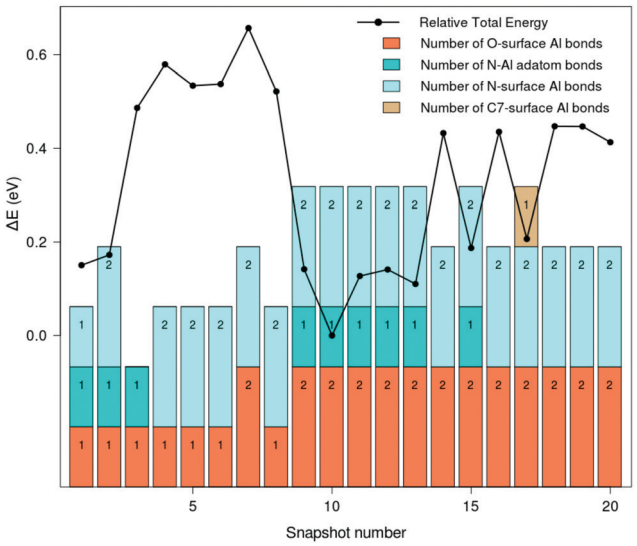

Fig. 8 Three **q** molecules adsorbed on Al–Al(111). Geometries optimised from 20 snapshots of MD1; relative total energies ΔE (in eV) in black (the reference is the energy of the geometry 10); number of bonds between O atoms and surface Al atoms in dark orange; number of bonds between N atoms and the Al adatom in green-blue; number of bonds between N atoms and surface Al atoms in light blue; number of bonds between C7 atoms and surface Al atoms in brown. Atoms a and atom b are considered bonded if $d_{a-b} < 2.3$ Å.

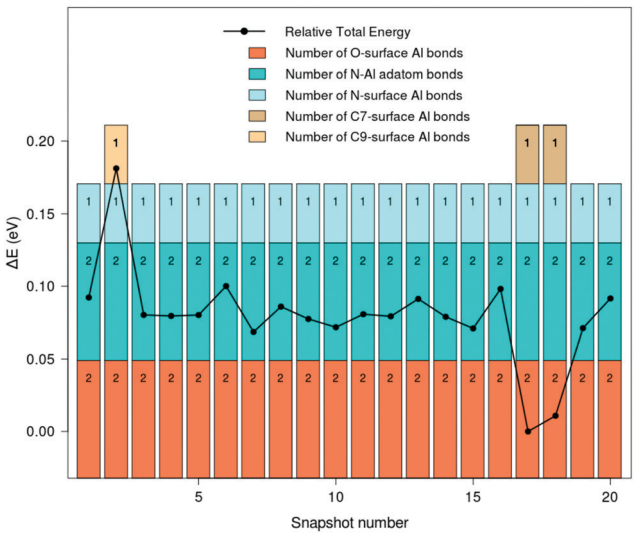

Fig. 9 Three **q** molecules adsorbed on Al–Al(111). Geometries optimised from 20 snapshots of MD2; relative total energies ΔE (in eV) in black (the reference is the energy of the geometry 17); number of bonds between O atoms and surface Al atoms in dark orange; number of bonds between N atoms and the Al adatom in green-blue; number of bonds between N atoms and surface Al atoms in light blue; number of bonds between C7 atoms and surface Al atoms in brown; number of bonds between C9 atoms and surface Al atoms in beige. Atoms a and atom b are considered bonded if $d_{a-b} < 2.3$ Å.

the C9 atom of the molecule **B** is in interaction with an Al atom of the surface. This destabilises the system, as the corresponding molecule is highly deformed (E_{def}^{molB} = 1.82 eV). For the more stable geometries (17 and 18), the formation of one C7–surface bond (2.192 ± 0.001 Å) stabilises the system.

2.2.2.3 Most stable geometries for three q molecules adsorbed on Al–Al(111). Geometry 10 from MD1 and geometry 17 from MD2 were reoptimised with more accurate computational parameters and Bader charge analyses were conducted on these structures. The geometry 17 from MD2 is the most stable one, the geometry 10 being 0.38 eV higher in energy. During the accurate optimisation of geometry 10, additional N–adatom and C7–Al bonds were formed. The structures of the systems are presented in Fig. 10. In both geometries, one molecule lies parallel to the metal surface, another is slightly tilted on the surface and the third one adopts an adsorption mode that is close to the perpendicular one. The interatomic distances between the oxygen and nitrogen atoms and the aluminium adatom are characteristic of covalent bonds. These latter are of the same order as the sum of the covalent radii for a simple bond ($r_{cov}^{O} + r_{cov}^{Al}$ = 0.63 + 1.26 = 1.89 Å; $r_{cov}^{N} + r_{cov}^{Al}$ = 0.71 + 1.26 = 1.97 Å) and largely smaller than the sum of the van der Waals radii ($r_{vdW}^{O} + r_{vdW}^{Al}$ = 1.52 + 1.84 = 3.36 Å; $r_{vdW}^{N} + r_{vdW}^{Al}$ = 1.55 + 1.84 = 3.39 Å). In the isolated **Alq$_3$** complexes, the O–Al distance is around 1.9 Å and the N–Al distance is around 2.1 Å. Thus the adsorption of 3 **q** molecules on Al–Al(111) leads to the formation of O–adatom and N–adatom bonds shorter than the ones observed in the free complex. In addition, one of the nitrogen atoms is not bonded to the adatom but to an Al surface atom (molecule **B**).

The molecule **A** is, in both structures, the one that has a quasi-perpendicular adsorption mode. It is in interaction with the Al adatom *via* its O and N atoms (O–Al and N–Al distances of 1.812/1.978 Å and 2.042/1.974 Å in geometries 10/17) and, in geometry 17, it is also in interaction with the surface *via* its O atom (1.947 Å).

The molecule **B** is the one that is positioned with a slight tilt relatively to the surface, the tilt being significantly larger in structure 10 than in structure 17. It is bonded to the adatom by its O atom (distance O–adatom: 1.887/1.882 Å for geometries 10/17), and to the surface *via* its O and N atoms, with distances between O and N and the surface Al atoms of 1.956/1.926 Å and 2.067/1.930 Å for geometries 10/17. In addition, a C7–surface bond is present in geometry 17 (2.185 Å).

Finally, the molecule **C**, which is parallel to the Al(111) surface, is bonded to the Al adatom both *via* its O and N atoms (distances O–adatom and N–adatom of 1.823/1.844 Å and 2.024/1.985 Å for geometries 10/17). In geometry 10, the N and C7 atoms are also bonded to surface Al atoms (distances N-surface Al atom and C7–surface Al atom of 2.183 Å and 2.153 Å).

The analysis of the electron population in geometries 10 and 17 is presented in Table 6 and gives information about the charge distribution within the systems and the bonding between the **q** molecules and the Al–Al(111) surface. In both geometries, the Al adatom is close to an Al^{III} oxidation state, with a charge of respectively +2.56 *e* and +2.48 *e* in geometries 10 and 17, similarly to the net charge of the Al atom in the isolated or adsorbed **Alq$_3$** complexes. A very strong electrons

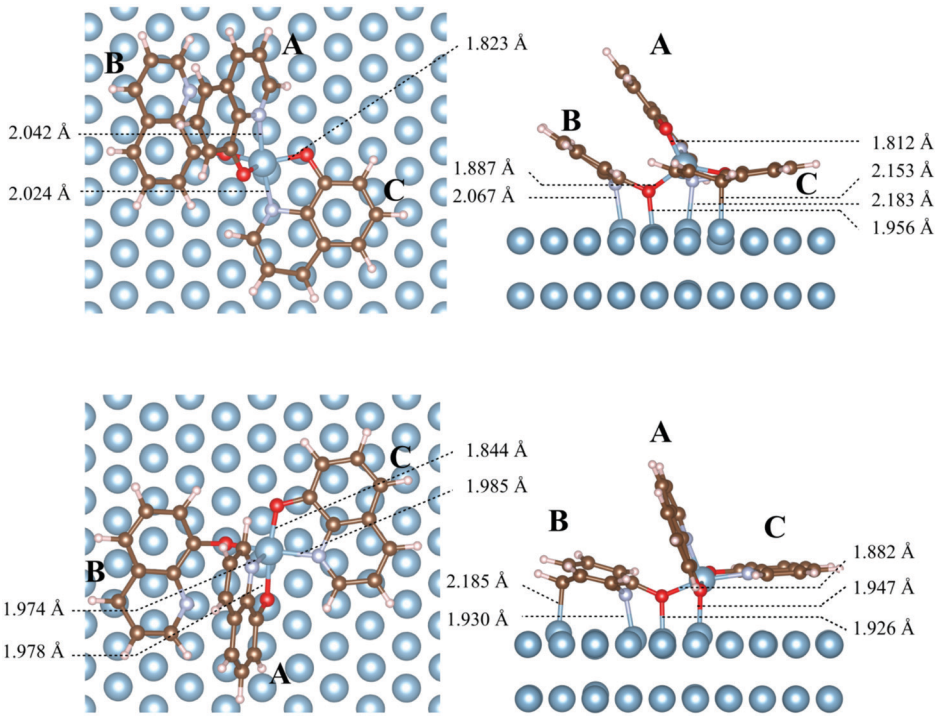

Fig. 10 Three **q** molecules adsorbed on Al–Al(111). Top: Geometry 10 from MD1. Bottom: Geometry 17 from MD2 (most stable form).

Table 6 **Alq$_3$** species on Al(111). First two lines: 3 **q** molecules adsorbed on Al–Al(111) in geometries 10 and 17. Last three lines: **Alq$_3$** complexes adsorbed on Al(111). Relative total energies (in eV, the reference is the energy of geometry 17); net charge on the Al adatom or on the Al atom in the complex; charge on molecules **A**, **B** and **C** (in *e*); distance from the Al adatom or from the Al atom in the complex to the Al(111) surface (in Å)

Species	ΔE	q_{Al}	Q_{molA}	Q_{molB}	Q_{molC}	dz_{Al}
Geometry 10	0.38	+2.56	−0.85	−1.25	−2.18	3.206
Geometry 17	0	+2.48	−0.97	−2.18	−1.25	2.738
mer/up	0.79	+2.44	−0.94	−1.26	−0.98	3.862
mer/down	0.94	+2.36	−1.26	−1.49	−1.25	3.897
fac/up	0.25	+2.45	−1.08	−1.19	−1.14	3.509

transfer occurs from the Al–Al(111) surface to the **q** molecules (respectively 4.28 *e* and 4.40 *e* for geometries 10 and 17). The electron gain redistribution is different for the three molecules and depends particularly on their direct bonding with the Al(111) surface. The molecule **A** has a charge of −0.85 *e* for the geometry 10 and −0.97 *e* for the geometry 17. Its perpendicular adsorption conformation makes a direct bonding with surface Al atoms difficult to form. However, one O–surface Al atom bond is observed in geometry 17 and the electron transfer is slightly higher. The **q** molecules bonded to the adatom and to Al(111) *via* their O (or N) and C7 atoms gains 2.18 *e*. It corresponds to **C** in geometry 10 and to **B** in geometry 17. The electron transfer to the third molecule, **B** in geometry 10 and **C** in geometry 17, is lower (1.25 *e*).

The adsorption energy of the three **q** molecules on Al–Al(111) is −13.08 eV in the most stable geometry located during our conformational exploration (geometry 17 MD2). To locally characterise the strength of the interactions within the 3**q**/Al–Al(111) system, interaction energies between different subparts of the system were computed and the corresponding values are summarised in Table 7, together with the deformation energies. For this stable species on the aluminium surface, the interaction energy between the three **q** molecules and the Al–Al(111) surface is −17.20 eV, evidencing a very strong bonding of the molecules on the Al–Al(111) surface.

As described above, in geometry 17, the molecules **A**, **B** and **C** have different adsorption topologies. Even if its adsorption geometry is close to a perpendicular mode, the molecule **A** interacts strongly with the rest of the system, with an interaction energy of −6.40 eV (with a contribution of 14% of the van der Waals interactions), and is slightly deformed with a deformation energy of 0.49 eV during the formation of the 3 **q**/Al–Al(111) species. Similarly, the molecule **C** is slightly deformed upon adsorption (deformation energy of 0.43 eV) because it is only directly bonded to the Al adatom and van der Waals contribution represents 22% of its interaction energy (−5.87 eV) with the rest of the system. This van der Waals contribution is mainly due to the parallel adsorption geometry of **C** and thus to interactions between the molecule and the Al–Al(111) surface (value of −1.11 eV for $E_{int}^{molC/Al-Al(111)}$(vdW)). The molecule **B** is the molecule that shows the strongest interaction with the rest of the system with an interaction energy of −6.91 eV, including van der Waals interaction of **B** with the molecule **A** and with the Al–Al(111) surface ($E_{int}^{molB/Al-Al(111)}$(vdW) = −1.23 eV). It is directly bonded with the surface and is thus strongly deformed upon adsorption (deformation energy of 2.03 eV).

To investigate the strength of the interaction of the Al(111) surface with the **Alq$_3$**-like species, the interaction energy

Table 7 Most stable geometry for three **q** molecules adsorbed on Al–Al(111): interaction energies between subparts of the system, van der Waals energy contribution and deformation energies (in eV)

Part 1	Part 2	$E_{int}^{part1/part2}$	$E_{int}^{part1/part2}$(vdW)	E_{def}^{part1}
mol**A** + mol**B** + mol**C**	Al–Al(111)	−17.20	−2.82	2.95
mol**A**	mol**B** + mol**C** + Al–Al(111)	−6.40	−0.91	0.49
mol**B**	mol**A** + mol**C** + Al–Al(111)	−6.91	−1.55	2.03
mol**C**	mol**A** + mol**B** + Al–Al(111)	−5.87	−1.30	0.43
mol**A**	Al–Al(111)	−4.56	−0.49	0.49
mol**B**	Al–Al(111)	−6.15	−1.23	2.03
mol**C**	Al–Al(111)	−4.78	−1.11	0.43
mol**A** + mol**B** + mol**C**	Al adatom	−13.48	−0.20	2.95
mol**A** + mol**B** + mol**C** + Al adatom	Al(111)	−6.23	−2.83	

between the three molecules (**A** + **B** + **C**) and the Al adatom, as in the isolated complex, and the interaction energy between the complex-like system (**A** + **B** + **C** + Al adatom) and the Al(111) surface are also presented in Table 7. The interaction energy between the three molecules (**A** + **B** + **C**) and the Al adatom has a value of −13.48 eV. It again demonstrates that the three molecules are strongly bonded to the Al atom, forming an **Alq$_3$** complex with a geometry that is nearly as stable as the optimised complex when isolated from the Al(111) surface ($E_{int}^{3mol/Al}$ = −15.13 ± 0.07 eV in that case). The interaction energy between the **Alq$_3$**-like species (**A** + **B** + **C** + Al adatom) and the Al(111) surface, with a value of −6.23 eV, evidences a strong adsorption of the complex on the Al(111) surface. This latter is significantly stronger that in the case of the direct adsorption on the Al(111) surface of the **Alq$_3$** species pre-formed in vacuum ($E_{int}^{cx/Al(111)}$ = −3.61 ± 0.49 eV).

The electron density variation $\Delta\rho$ occurring during the adsorption of the 3 **q** molecules on the Al–Al(111) surface is presented in Fig. 11 for geometry 17. A large redistribution of the electron density is observed and the electron accumulation between the molecules, the adatom and the aluminium surface confirms the formation of direct O–Al, N–Al and C–Al bonds. Thanks to this electron excess zone between the molecules, the Al adatom and the Al(111) surface, and the strong electrons transfer from the Al–Al(111) surface to the molecules highlighted above by Bader analysis, the bonding of the molecules with the metal atoms can be characterised as iono-covalent.

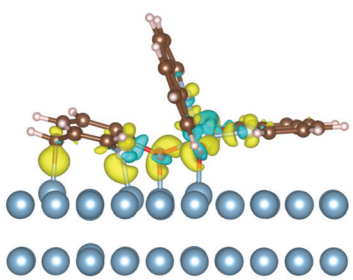

Fig. 11 Electron density variation upon adsorption for three **q** molecules adsorbed on Al–Al(111). Isosurface value: −0.0675/+0.0675 *e* Å^{-3}; yellow (blue): electron excess (deficit) regions.

2.2.3 Discussion. The direct adsorption of **Alq$_3$** complexes on an Al(111) surface and the adsorption of three **q** molecules on an Al–Al(111) surface can only be compared in term of total energy and the relative total energies ΔE are presented in Table 6. The system formed by the adsorption of three **q** molecules on an Al–Al(111) surface is the most stable one. The **Alq$_3$** complex adsorbed on Al(111) in the *fac/up* configuration is 0.25 eV higher in energy followed by the *mer/up* and *mer/down* configurations at 0.79 and 0.94 eV, respectively. In the most stable system, the Al adatom is at 2.738 Å from the Al(111) surface, *i.e.* about 1 Å smaller than the distances between the Al atom of the complex and the Al(111) surface in the *mer/up*, *mer/down* and *fac/up* geometries. The transition from the direct adsorption of **Alq$_3$** complexes to the most stable configuration (geometry 17) would therefore require a significant structural reorganisation. The charge on the central aluminium atom is very similar in the four structures, the Al atom being in strong interaction with the **q** molecules with an oxidation state close to Al^{III}. With regard to the formation of **Alq$_3$** complex layers on aluminium surfaces, it is conceivable that these two pathways may exist depending, *inter alia*, on the species present in solution (presence of free **q** or not), on the number of defects present on the aluminium surface, and on the activation barriers in play in the different pathways. The determination of these latter will be the purpose of forthcoming studies.

A very interesting point highlighted by this study is that the charge transferred from the metal surface to the metal–organic complexes is substantial, resulting in negatively charged complexes. This charge distribution raises the question whether such charge distribution is also observed at high coverage, *i.e.* in metal–organic layers covering aluminium surfaces. If this is the case and if the coverage of the metal by the organic layer is total, it could be envisaged that electrostatic repulsion could be part of the corrosion inhibition mechanism, as a globally negatively charged surface layer would repel the anions responsible for corrosion initiation.

3 Conclusions

The atomic scale structure of **Alq$_3$** complexes adsorbed on Al(111) surfaces has been investigated following two scenarios:

the direct adsorption of **Alq$_3$** complexes pre-formed in vacuum on flat Al(111) surfaces, or the sequential adsorption of three molecules on a defective Al(111) surface, on which Al adatoms are present. During the **Alq$_3$** formation in vacuum, each addition of a **q** molecule on the Al atom stabilises the system, the oxidation state of the Al atom evolving from Al^{I} in **Alq** to Al^{III} in **Alq$_2$** and **Alq$_3$**. Two conformations of the **Alq$_3$** complex were investigated in vacuum and both were subsequently deposited on a flat Al(111) surface. The **Alq$_3$** complex bonding to the surface is strong, with adsorption energies between −1.52 and −2.21 eV. This deposition lead to the formation of O–Al, N–Al and C–Al bonds between the **q** molecules of the complex and the Al(111) surface and to a significant electron transfer from the surface to the complexes ranging from 0.73 to 1.57 *e*. The formation of **Alq$_3$** complex *via* the sequential adsorption of **q** molecules on an Al adatom present on the aluminium surface was investigated thanks to AIMD runs, which allowed the conformational space to be explored. The obtained adsorption conformations are more stable than the one obtained from direct adsorption on Al(111) of pre-formed **Alq$_3$** complexes in vacuum. In the most stable conformation, two **q** molecules are almost parallel to the Al surface and the third one is almost perpendicular, the three molecules being bonded to the Al adatom but only two being bonded to the surface. The electron transfer from the Al–Al(111) surface is 4.40 *e* and is distributed unevenly on the three molecules with an enhanced transfer (2.18 *e*) to the molecule most bonded to the surface, *via* its O, N and C atoms.

It is conceivable that the two studied pathways leading to the formation of **Alq$_3$** layers on aluminium surfaces could coexist. Parameters such as the presence in solution of free **q** molecules, the number of defects on the aluminium surface, or the determination of the activation barriers at play in the different pathways would allow to go further in the comparison of these pathways. Based on structures, energetics and charge distributions data, one can conclude that the bonding between the **q** molecules and the Al atoms has an iono-covalent nature. The nature of this interaction will be studied in more detail in a forthcoming paper presenting a topological study of these bonds and the effect of the solvent on these adsorption modes will be evaluated. The significant charge transferred from the metal surface to the metal–organic complexes lead to the open question of a possible electrostatic contribution to corrosion inhibition mechanisms.

Conflicts of interest

There are no conflicts to declare.

Acknowledgements

This work was granted access to the HPC resources of CALMIP supercomputing center (allocation 2019-p12174) and of GENCI supercomputing center (allocation A0070910602 at CINES). It was also supported by the French Ministry of Higher Education and Research [YB, PhD grant].

Notes and references

1 F. C. F. Barros, F. W. Sousa, R. M. Cavalcante, T. V. Carvalho, F. S. Dias, D. C. Queiroz, L. C. G. Vasconcellos and R. F. Nascimento, *Clean*, 2008, **36**, 292–298.
2 M. Muccini, M. A. L. K. Kenevey, R. Zamboni, N. Masciocchi and A. Sironi, *Adv. Mater.*, 2004, **16**, 861–864.
3 C. F. R. A. C. Lima, R. J. S. Taveira, J. C. S. Costa, A. M. Fernandes, A. Melo, A. M. S. Silva and L. M. N. B. F. Santos, *Phys. Chem. Chem. Phys.*, 2016, **18**, 16555–16565.
4 A. Curioni, M. Boero and W. Andreoni, *Chem. Phys. Lett.*, 1998, **294**, 263–271.
5 I. C. Avetissov, A. A. Akkuzina, R. I. Avetisov, A. V. Khomyakov and R. R. Saifutyarov, *CrystEngComm*, 2016, **18**, 2182–2188.
6 C. W. Tang and S. A. VanSlyke, *Appl. Phys. Lett.*, 1987, **51**, 913–915.
7 Z. Shen, P. E. Burrows, V. Bulovic, S. R. Forrest and M. E. Thompson, *Science*, 1997, **276**, 2009–2011.
8 A. Moliton, W. Rammal and B. Lucas, *Eur. Phys. J.: Appl. Phys.*, 2006, **33**, 175–182.
9 L. Garrigues, N. Pébère and F. Dabosi, *Electrochim. Acta*, 1996, **41**, 1209–1215.
10 S. V. Lamaka, M. L. Zheludkevich, K. A. Yasakau, M. F. Montemor and M. G. S. Ferreira, *Electrochim. Acta*, 2007, **52**, 7231–7247.
11 S. Marcelin and N. Pébère, *Corros. Sci.*, 2015, **101**, 66–74.
12 H. Soliman, *Corros. Sci.*, 2011, **53**, 2994–3006.
13 A. C. Balaskas, M. Curioni and G. E. Thompson, *Surf. Interface Anal.*, 2015, **47**, 1029–1039.
14 I. G. Hill, A. J. Makinen and Z. H. Kafabi, *Appl. Phys. Lett.*, 2000, **77**, 1825–1827.
15 D. Ino, K. Watanabe, N. Takagi and Y. Matsumoto, *Phys. Rev. B: Condens. Matter Mater. Phys.*, 2005, **71**, 115427.
16 Z. Wang, A. Pronschinske and D. B. Dougherty, *Org. Electron.*, 2011, **12**, 1920–1926.
17 J. Zhang, P. Chen, B. Yuan, W. Ji, Z. Cheng and X. Qiu, *Science*, 2013, **342**, 611–614.
18 A. Droghetti, P. Thielen, I. Rungger, N. Haag, N. Großmann, J. Stöckl, B. Stadtmüller, M. Aeschlimann, S. Sanvito and M. Cinchetti, *Nat. Commun.*, 2016, **7**, 12668–12677.
19 T. Mori, H. Fujikawa, S. Tokito and Y. Taga, *Appl. Phys. Lett.*, 1998, **73**, 2763–2765.
20 A. Curioni and W. Andreoni, *Synth. Met.*, 2000, **111-112**, 299–301.
21 M. G. Mason, C. W. Tang, L.-S. Hung, P. Raychaudhuri, L. Yan, Q. T. Le, Y. Gao, S.-T. Lee, L. S. Liao, L. F. Cheng, W. R. Salaneck, D. A. dos Santos and J. L. Bredas, *J. Appl. Phys.*, 2001, **89**, 2756–2767.
22 T. Yokoyama, D. Yoshimura, E. Ito, H. Ishii, Y. Ouchi and K. Seki, *Jpn. J. Appl. Phys.*, 2003, **42**, 3666–3677.
23 S. Yanagisawa and Y. Morikawa, *Chem. Phys. Lett.*, 2006, **420**, 523–528.

24 S. Yanagisawa, K. Lee and Y. Morikawa, *J. Chem. Phys.*, 2008, **128**, 244704.
25 Y.-P. Wang, X.-F. Han, Y.-N. Wu and H.-P. Cheng, *Phys. Rev. B: Condens. Matter Mater. Phys.*, 2012, **85**, 144430.
26 S. Yanagisawa and Y. Morikawa, *J. Phys.: Condens. Matter*, 2009, **21**, 64247–64259.
27 S. Peljhan, J. Koller and A. Kokalj, *J. Phys. Chem. C*, 2014, **118**, 933–943.
28 N. Kovacevic, I. Milosev and A. Kokalj, *Corros. Sci.*, 2015, **98**, 457–470.
29 Y. Wang, N. S. Hush and J. R. Reimers, *J. Am. Chem. Soc.*, 2007, **129**, 14532–14533.
30 F. Chiter, C. Lacaze-Dufaure, H. Tang and N. Pébère, *Phys. Chem. Chem. Phys.*, 2015, **17**, 22243–22258.
31 F. Chiter, M.-L. Bonnet, C. Lacaze-Dufaure, H. Tang and N. Pébère, *Phys. Chem. Chem. Phys.*, 2018, **20**, 21474–21486.
32 A. Kokalj, S. Peljhan, M. Finšgar and I. Milošev, *J. Am. Chem. Soc.*, 2010, **132**, 16657–16668.
33 N. Kovacevic and A. Kokalj, *J. Phys. Chem. C*, 2011, **115**, 24189–24197.
34 N. Kovacevic and A. Kokalj, *Corros. Sci.*, 2013, **73**, 7–17.
35 A. Kokalj, S. Peljhan and J. Koller, *J. Phys. Chem. C*, 2014, **118**, 944–954.
36 M. Poberznik, D. Costa, A. Hemeryck and A. Kokalj, *J. Phys. Chem. C*, 2018, **122**, 9417–9431.
37 C. Kittel, *Introduction to Solid State Physics*, Wiley, 1996.
38 G. Kresse and J. Hafner, *Phys. Rev. B: Condens. Matter Mater. Phys.*, 1993, **47**, 558–561.
39 G. Kresse and J. Furthmüller, *Phys. Rev. B: Condens. Matter Mater. Phys.*, 1996, **54**, 11169–11186.
40 G. Kresse and J. Furthmuller, *Comput. Mater. Sci.*, 1996, **6**, 15–50.
41 J. P. Perdew, K. Burke and M. Ernzerhof, *Phys. Rev. Lett.*, 1996, **77**, 3865–3868.
42 J. P. Perdew, K. Burke and M. Ernzerhof, *Phys. Rev. Lett.*, 1997, **78**, 1396.
43 P. E. Blöchl, *Phys. Rev. B: Condens. Matter Mater. Phys.*, 1994, **50**, 17953–17979.
44 G. Kresse and D. Joubert, *Phys. Rev. B: Condens. Matter Mater. Phys.*, 1999, **59**, 1758–1775.
45 S. Grimme, *J. Comput. Chem.*, 2006, **27**, 1787–1799.
46 S. Grimme, J. Antony, S. Ehrlich and H. Krieg, *J. Chem. Phys.*, 2010, **132**, 154104.
47 H. J. Monkhorst and J. D. Pack, *Phys. Rev. B: Solid State*, 1976, **13**, 5188–5192.
48 M. Methfessel and A. T. Paxton, *Phys. Rev. B: Condens. Matter Mater. Phys.*, 1989, **40**, 3616–3621.
49 M. P. Allen and D. J. Tildesley, *Computer Simulation of Liquids*, Oxford University Press, 1991.
50 W. G. Hoover, A. J. C. Ladd and B. Moran, *Phys. Rev. Lett.*, 1982, **48**, 1818–1820.
51 D. J. Evans, *J. Chem. Phys.*, 1983, **78**, 3297–3302.
52 W. Tang, E. Sanville and G. Henkelman, *J. Phys.: Condens. Matter*, 2009, **21**, 084204.
53 H. Li, F. Zhang, Y. Wang and D. Zheng, *Mater. Sci. Eng., B*, 2003, **100**, 40–46.
54 A. K. Saxena, *Synth. React. Inorg. Met.-Org. Chem.*, 1999, **29**, 1747–1767.
55 M. Colle, R. E. Dinnebier and W. Brütting, *Chem. Commun.*, 2002, 2908–2909.